

Role of Water in the Phase Transformations Observed in Solutions of a Rigid Polymer

Yachin Cohen* and Eytan Cohen

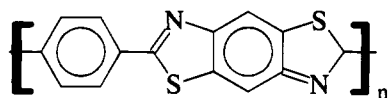
Department of Chemical Engineering, Technion—Israel Institute of Technology, Haifa 32000, Israel

Received December 20, 1992; Revised Manuscript Received February 28, 1995[®]

ABSTRACT: Formation of crystal solvate phases was investigated in solutions of the rigid polymer poly(*p*-phenylene benzobisthiazole) (PBZT) in methanesulfonic acid (MSA), with particular emphasis on the role of water in inducing the phase transitions. Crystal solvates are crystalline solids which contain both polymer and solvent molecules in the unit cell. A ternary phase diagram for the PBZT/MSA/water system was determined at room temperature, and the following phases were identified: isotropic phase, nematic liquid crystalline phase, and crystal solvate forms I and II. These phases were recognized visually, as well as by light microscopy and analysis of X-ray diffraction. In the suggested model of the form I crystal solvate, four acid anions are complexed to a protonated PBZT repeat unit, with two additional acid molecules, in a unit cell. Absorption of moisture by the solution induces precipitation of the form I phase by generating an excess of acid anions beyond the solubility product. The form II crystal solvate was formed after deprotonation of the polymer, when the molar concentration of penetrating water equals the molar concentration of the free acid.

Introduction

Fibers and films fabricated from rigid polymers exhibit excellent mechanical properties, examples of which are the aramid fibers of poly(*p*-phenylene terephthalamide) (PPTA) available from commercial sources and the heteroaromatic fibers developed by the U.S. Air Force Ordered Polymers Program. An example of the latter is poly[*p*-phenylene(benzo[1,2-*d*:4,5-*d'*]bisthiazole-2,6-diyl)] (PBZT), from which fibers having tensile modulus and strength exceeding 300 and 3 GPa, respectively, have been reported.^{1,2} The chemical structure of PBZT is shown below:



Attainment of exceptional tensile properties is due to a high degree of orientational order of the rigid chain achieved during processing of the fibers. Due to the rigidity and regularity of the molecular structure along the chain, these polymers can be processed only from solutions in strongly interacting solvents. These include strong acids which protonate the polymer, so that solubility is due to electrostatic repulsion of the rigid polycations. Recently, solubility in polar organic solvents in the presence of strong Lewis acids has been reported.^{3,4}

In a typical process for spinning rigid polymer solutions, a liquid crystalline solution is extruded through a spinnerette separated by a narrow air gap from a coagulation bath. Solidification of the solution stream occurs in the coagulation bath by the action of a nonsolvent, typically water. Beltsios and Carr presented a critical evaluation of mechanisms for formation of the solid phase when the oriented solution is coagulated.⁵ The major effects are diffusion of water into the solution stream, deprotonation of the polymer cations, crystallization of the rigid polymer, and removal of the diluted solvent. Studies of the morphology^{6,7} which

develops during coagulation of the oriented PBZT solution have shown the formation of a network of microfibrils, the width of which is less than 10 nm. These studies indicate that the basic structural elements of the solid fiber are set during coagulation, pointing to the importance of understanding the phase transformations in the polymer/solvent/coagulant system.

The crystal structure of PBZT has been studied in detail.^{8,10} Much less is known about its crystal solvate phases. These result from cocrystallization of the polymer with its solvent as an ionic complex of protonated polymer cations and acid anions.¹¹ The temperature–composition phase diagram has been reported for PTTA/sulfuric acid, and the structure of the crystal solvate in this system has been determined.¹² In early studies on PBZT solutions, crystal solvate phases were shown to form in its solutions in methanesulfonic acid (MSA)^{13,14} and poly(phosphoric acid) (PPA).^{15,17} Solutions in PPA are the polymerization medium for PBZT¹⁸ and are used directly in the spinning process. The studies revealed that two types of crystal solvate phases exist in this system. The first type, denoted form I, is a highly ordered crystalline phase, exhibiting three-dimensional order, usually absent in the PBZT crystalline state. It appears at low moisture uptake by the PBZT/PPA solution, has a light-green color, and is considered as a cocrystal containing protonated PBZT cations and acid anions. At higher moisture uptake or when the solution stream is coagulated in 85% phosphoric acid, another type of crystal solvate phase having a reddish color appears. It is denoted form II and is much less ordered than the form I crystal solvate. Studies of the phase transitions by X-ray diffraction using synchrotron radiation¹⁷ showed that form I melts to a liquid state at about 70 °C and recrystallizes upon cooling. On the other hand, the form II crystal solvate exhibits an irreversible crystal–crystal transition at elevated temperatures, above 200 °C. A quantitative evaluation of the phase diagram was not possible due to the extremely high viscosity of PBZT/PPA solutions and the low moisture contents which induce the transitions.

The objective of this study was to establish quantitatively the formation of the two crystal solvate forms in the ternary rigid polymer/acid solvent/water system.

* To whom correspondence should be addressed.

[®] Abstract published in *Advance ACS Abstracts*, April 1, 1995.

In particular, the role of water in these transitions, involving proton transfer equilibria, is sought. Solutions of a low molecular weight PBZT in MSA were used in this study. These solutions are more manageable due to their lower viscosity and exhibit the phase transitions at a higher water content compared to the PPA solutions.

Experimental Section

End-capped, low molecular weight PBZT was synthesized by J. Wolfe at the Stanford Research Institute. The intrinsic viscosity of 250 cm³/g (in MSA at 25 °C) indicates a molecular weight of approximately 11 000.¹⁹ The PBZT flakes were slurried in 1 M NaOH, then thoroughly washed with distilled water, and dried in a vacuum oven. MSA (Fluka, analytical grade) was distilled under vacuum. PBZT/MSA mixtures were stirred at 70 °C for a few hours until homogeneous solutions having a dark green color were obtained. All sample preparations were carried out in a glovebag under dry nitrogen. Slow absorption of water into the solutions was performed by placing open vials in a desiccator containing an open beaker of water for periods of time ranging from a few hours to several days. The temperature of the experiments was 20 ± 2 °C. Phase transitions were determined by visual inspection of the color change during absorption of moisture. Transition to the form I crystal solvate was indicated by a light-green color which persisted after stirring at 70 °C to homogenize the solution and cooling back to 20 °C. The transition to the form II crystal solvate was determined in a similar way by observation of a red color in the solid phase.

Wide-angle X-ray diffraction patterns were recorded on flat film (Osray C) in a Warhus camera with 0.025 in. pinholes (Blake), using Ni-filtered Cu K α radiation from a sealed-tube generator (Philips PW1730). The camera was equipped with a heating cell and temperature controller (Omron). The sample to detector distance was 53.3 mm, and α -alumina powder was used for calibration. The extremely high X-ray absorption by MSA (linear absorption coefficient 54.7 cm⁻¹) made it necessary to expose very thin regions of the samples. Further care was needed due to the extreme moisture sensitivity of the crystal solvates. Samples were sealed in thin-walled glass capillaries 2 mm in diameter (Müller). Regions where a thin portion of the sample covered the capillary wall were selected for diffraction. Exposure times were 8–70 h.

Observations by optical microscopy were performed with an Olympus BH-2 model with crossed polarizers and a Mettler FP-5 hot stage. Samples were placed between the glass slide and a cover slip in a glovebag and were sealed with epoxy glue. Alternatively, a drop of solution between a glass slide and a cover slip was allowed to gradually absorb moisture from the atmosphere. For differential scanning calorimetry measurements (DSC) a Mettler TA3000 instrument was used. Flame-sealed glass sample containers (Mettler) were used for the acid-containing samples. Heating and cooling rates of 10 °C/min were employed. Spectroscopic measurements in the 350–800 nm range were performed with a Pye-Unicam SP8-250.

Results and Discussion

The most distinct indications of phase transitions in the PBZT/MSA solutions, due to absorption of water, were the color changes.²⁰ The original solution had a dark green color, which transformed to light green upon precipitation of the form I crystal solvate, then to red when a transition to form II occurred, and finally to the yellow-orange color of the solid PBZT precipitate upon immersion in water. These transitions were evident in the visible-light spectra obtained from the different phases. Spectrum a in Figure 1 was obtained from a 2% (w/w) PBZT/MSA solution. Following absorption of moisture to a composition containing 1.8% PBZT and 8.8% water, the form I crystal solvate developed, exhibiting spectrum b in Figure 1. Spectrum c was

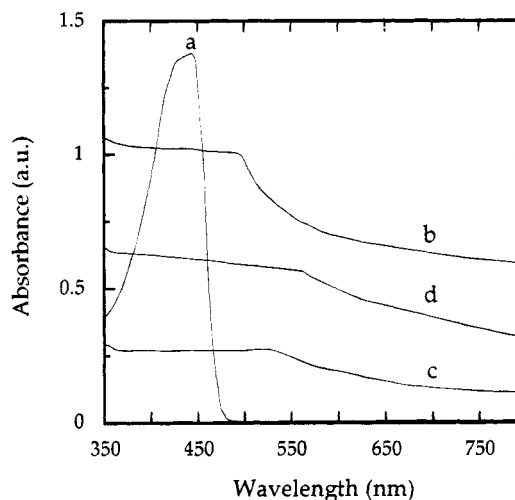


Figure 1. Visible-light absorbance spectra of a PBZT/MSA solution at increasing water content: (a) the anhydrous solution; (b) form I crystal solvate; (c) form II crystal solvate; (d) crystalline PBZT.

obtained from the form II crystal solvate after further absorption of moisture to a composition containing 1.7% PBZT and 14.8% water. After washing with a large quantity of water, spectrum d was obtained from the solid mass of the precipitated PBZT crystals. The prominent feature in Figure 1 is the shift in the absorption edge to longer wavelengths as more water is introduced into the system. This is in accord with earlier findings by Hsu and co-workers²¹ and is related to the effect of protonation on the degree of conjugation along the PBZT chain. Full protonation in the MSA solution reduces the conjugation resulting in the dark green color. A shift to the red is already noticeable in the spectrum of the form I crystal solvate, suggesting a decrease in the strength of the protonation interaction during precipitation of the form I crystal. The green color, though, is an indication that the polymer is still protonated in this state. A further shift to the red is noticed upon transition to the form II crystal solvate and the final crystalline PBZT phase. Their reddish color is an indication that the polymer is deprotonated, exhibiting the full conjugation length attainable in the PBZT structure.

The amount of water which needs to be absorbed for precipitation of the form I phase is a strongly decreasing function of the polymer concentration. The water concentration at the onset of precipitation of the form I crystal solvate is shown in Figure 2 as a function of the PBZT concentration. The role of water in inducing this phase transition is considered in terms of proton transfer equilibria and the structure of the form I phase. As in the case of several other crystal solvate phases reported, such as PPTA/sulfuric acid^{11,12} and PBZT/PPA,^{15,17} the form I phase is viewed as a cocrystal of protonated polymer cations and solvent anions, with the possibility of additional free acid molecules incorporated into the unit cell. The model for formation of this phase is the following: absorption of water produces more solvent anions by deprotonation of MSA until the solubility product of the protonated polymer and the acid anions is surpassed. This results in precipitation of the ionic "salt" by cocrystallization of protonated PBZT with MSA anions.

Formation of the form I crystal solvate is evaluated in terms of the following equilibrium reactions: protonation of the polymer repeat unit, where the degree of

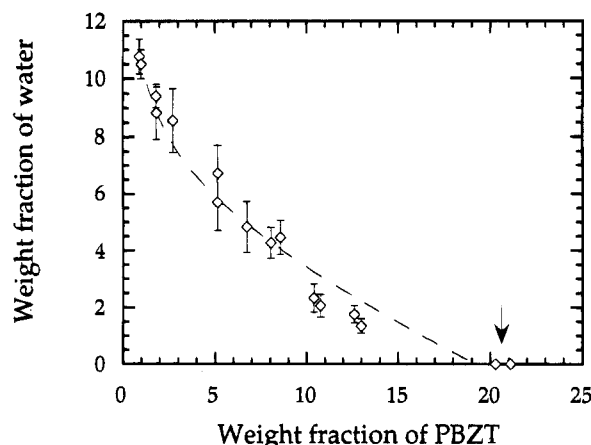
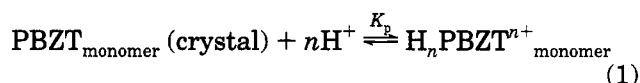
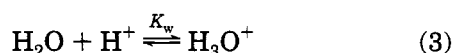


Figure 2. Water concentration at the onset of precipitation of the form I crystal solvate as a function of the PBZT concentration. Dashed line: fit of eq 8 with one adjustable parameter, the solubility product K_{xs} . Arrow indicates the form I phase at anhydrous conditions.

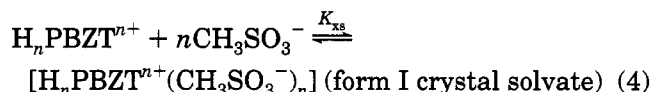
protonation is a variable n and the equilibrium constant is K_p :



dissociation of the acid solvent (equilibrium constant K_a) and protonation of water.



The solubility limit of the form I crystal solvate is defined by the solubility product K_{xs} :



By the law of mass action, the crystal solvate phase will form when the product of the concentrations of the MSA anions and the PBZT cations exceeds the solubility limit. The condition for the onset of precipitation of the form I phase is thus

$$[\text{H}_n\text{PBZT}^{n+}][\text{CH}_3\text{SO}_3^-]^n = K_{xs} \quad (5)$$

where the square brackets denote concentration, in moles/liter, of protonated PBZT monomer repeat units and MSA anions.

Considering the absorption of a small amount of water such that there still exists an excess of free (protonated) acid molecules in solution, we may make the following approximations: all water molecules absorbed are protonated at the expense of the free acid, creating more acid anions; the polymer remains protonated at the stoichiometric ratio of n protons per monomer repeat unit. By these assumptions the only relevant equilibrium constant is the solubility product K_{xs} , and the following equations hold:

$$[\text{H}_n\text{PBZT}^{n+}] = P_0/V_{\text{sol}} \quad (6)$$

$$[\text{CH}_3\text{SO}_3^-] = (nP_0 + W)/V_{\text{sol}} \quad (7)$$

where P_0 is the initial molar quantity of PBZT used, W is the molar quantity of absorbed moisture, and V_{sol} is the total solution volume. Concentration units were converted to weight fraction of PBZT and water in order to compare with the experimental measurements. To this end an average solution density of 1.476 g/cm^3 was taken and assumed to be constant. The relationship between the weight fractions of PBZT and water at the onset of precipitation of the form I crystal solvate, W_p and W_w , respectively, can be obtained by substituting eqs 6 and 7 into eq 5:

$$W_w = 1.22 \times 10^{-2} \left(0.1802 \frac{K_{xs}}{W_p} \right)^{1/n} - 0.0677nW_p \quad (8)$$

Equation 8 was fit to the experimental data using a multivariate least-squares analysis with the stoichiometry n and the solubility constant K_{xs} as fit parameters. A value of 3.89 was obtained for the stoichiometry, which is reasonably close to 4 protons per PBZT repeat unit, implying protonation on all nitrogen and sulfur atoms. Taking 4 as the protonation stoichiometry, the fit of eq 8 to the experimental data, with K_{xs} as a single fit parameter, is shown as the dashed line in Figure 2. The good fit to the data gives support to the model by which precipitation of the form I crystal solvate is essentially a "salting out" of the PBZT/MSA complex, induced by excess MSA anions created when water is absorbed. A value of $354 (\text{mol/L})^5$ is obtained for the solubility constant.

Crystallization of the form I crystal solvate when moisture is gradually absorbed by a dilute solution was followed by optical microscopy using crossed polarizers. A 2% (w/w) PBZT solution in MSA was placed between a glass slide and a cover slip and allowed to absorb moisture from ambient atmosphere. Initial precipitation occurred at the edges of the solution droplet, and with time spherulites appeared at the center of the sample. Growth of these crystal solvate spherulites as a function of time is shown in Figure 3. A number of spherulites appeared to grow at the same time, nucleating within the first few minutes of observation, such as the ones numbered 1–3 in Figure 3. We consider the formation of these spherulites to be due to heterogeneous nucleation on dust particles or defects in the glass surface. Spherulitic crystallization of PBZT/MSA crystal solvates has been reported previously.^{13,14} Imaging by transmission electron microscopy revealed the lamellae within the spherulites, with a characteristic width comparable to the length of the PBZT chains. This is of course reasonable in view of the rigidity of the PBZT chain which prohibits chain folding. As more water diffused into the sample, additional spherulites developed, such as the one marked 4 in Figure 3. These spherulites were formed continuously in what seemed to be homogeneous nucleation. This may be explained by the fact that as more water is absorbed, the excess MSA anions created increase the supersaturation of the solution. The linear growth rate of the initial spherulites (1–3 in Figure 3) is about the same, having a value of about $0.22 \mu\text{m/min}$ in the first hour. The growth rate of the spherulites nucleated later was slower. That of spherulite 4 in Figure 3 was measured to be $0.14 \mu\text{m/min}$ in its first hour of growth. This difference is most likely due to the lower PBZT concentration in the vicinity of this spherulite, depleted by growth of the spherulites nucleated earlier. This suggests that spherulite growth is not controlled by secondary nucleation

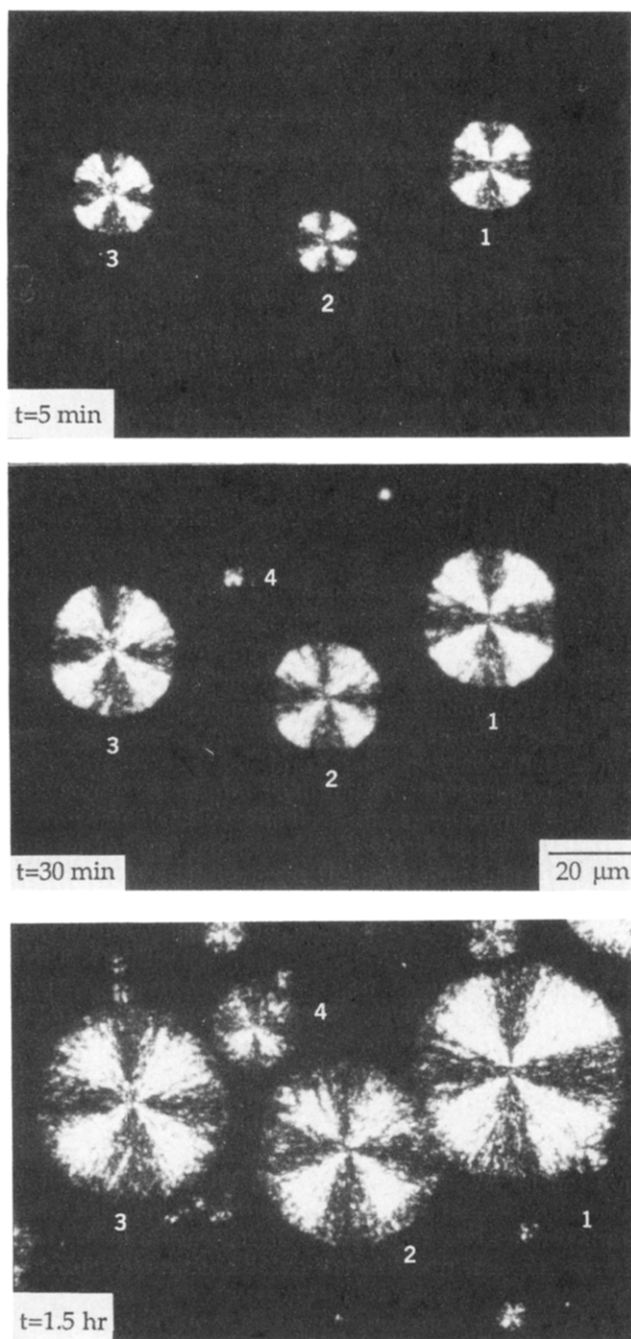


Figure 3. Growth of crystal solvate spherulites in a 2% (w/w) PBZT/MSA solution absorbing atmospheric moisture at 20 °C as a function of time.

but rather by diffusion of the rigid polymers to the crystal growth front.

The form I crystal solvate phase precipitates from solution at moderate absorption of moisture, as shown in Figure 2. At higher moisture contents, the precipitate changes in color to a reddish tint, which we denote the form II crystal solvate phase. The water content at the onset of this transition as a function of the PBZT concentration is shown in Figure 4. We interpret this transition as the onset of deprotonation of the PBZT polycations, which is brought about by the increasing water content. As a first approximation we consider the onset of this transition as the point where there are no longer any acid molecules in the system from which a proton can be transferred to incoming water molecules. Therefore the molar quantity of water absorbed at the point of transition (W_2) equals the molar quantity of free

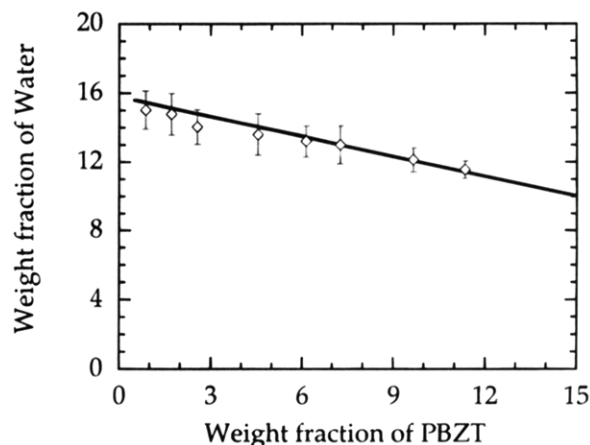


Figure 4. Water concentration at the transition to the form II crystal solvate as a function of the PBZT concentration. Solid line: fit of eq 10 with no adjustable parameters.

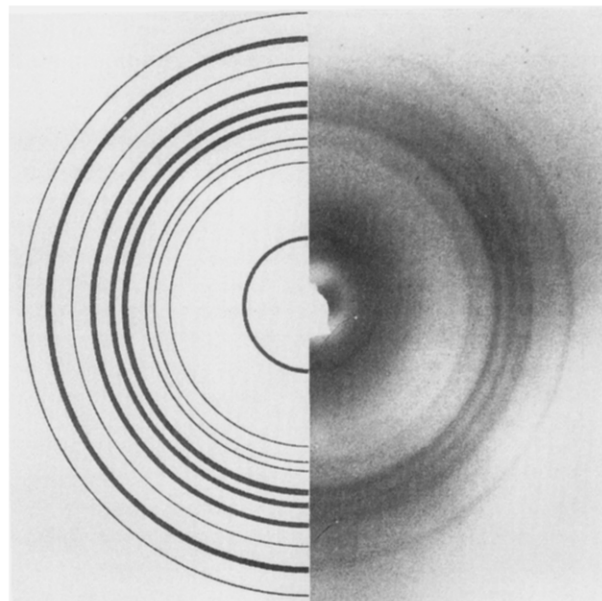


Figure 5. Diffraction pattern of the form I crystal solvate containing 20.3% (w/w) PBZT and 79.7% MSA at 20 °C.

acid molecules, which can be related to the initial molar quantities of MSA (A_0) and PBZT (P_0) as follows:

$$W_2 = A_0 - 4P_0 \quad (9)$$

Equation 9 implies a degree of protonation of 4 per PBZT repeat unit, as discussed above. Converting eq 9 to concentration units of weight fraction for comparison with the experimental measurements results in

$$W_w = 0.1579 - 0.3858W_p \quad (10)$$

Figure 4 shows that eq 10 provides a good fit of the experimental data, without any adjustable parameter. This supports the model by which the onset of the transition to the form II phase is due to deprotonation of the PBZT polycations.

The diffraction pattern of the form I crystal solvate, obtained from a sample containing 20.3% (w/w) PBZT in dry MSA at 20 °C is shown in Figure 5. The spacings of the observed reflections are listed in Table 1. A monoclinic unit cell, the dimensions of which are $a = 0.540$ nm, $b = 0.616$ nm, $c = 1.199$ nm, and $\gamma = 107^\circ$, was fit using the computer program TREOR 90. Assignment of Miller indices and the calculated spacings

Table 1. *d*-Spacings of Reflections from the Form I Crystal Solvate (Unit Cell: *a* = 0.540 nm, *b* = 0.616 nm, *c* = 1.199 nm, $\gamma = 107^\circ$)

obsd spacing, nm	calcd spacing, nm	index
1.199 strong	1.199	001
0.598	0.599	002
	0.589	010
0.529	0.529	011
0.516	0.516	100
	0.474	101
0.461 strong	0.461	110
	0.430	111
0.420 strong	0.420	012
0.399 strong	0.399	003
	0.391	102
0.368	0.365	112
0.342 strong	0.342	110
	0.331	013
	0.329	111
	0.316	103
0.300	0.300	004

are also listed in Table 1. The *c*-axis dimension of the unit cell equals the length of the PBZT repeat unit and is therefore denoted the chain axis direction. The diffraction pattern from the form II phase exhibited only two broad reflections centered at spacings of 0.497 and 0.343 nm. It is thus not possible to deduce a unit cell for this phase. When the sample of the form I crystal solvate containing 20.3% PBZT was heated to 150 °C, its color changed from light green to red, which indicates deprotonation of the polymer. The diffraction pattern at 150 °C, shown in Figure 6, is different from that of the form I phase of the same sample at 20 °C, which was shown in Figure 5. At 150 °C five diffraction rings can be observed at the following spacings: 1.467, 1.181, 1.020, 0.510, and 0.347 nm. Both color and diffraction pattern reverted to the original state upon cooling back to room temperature. This phase transformation was also evident by DSC as shown in Figure 7. An endothermic transition is observed at 131 °C upon heating, and an exothermic transition appears at 71 °C upon cooling. The reason for the large hysteresis between heating and cooling cycles is not clear.

The number of acid molecules associated with each PBZT repeat unit in the crystal structure is an important characteristic of the form I phase. The small number of observed reflections and the lack of reliable intensity measurements, due to absorption by MSA, prevent accurate determination of the crystal structure. However, some information can be estimated from considerations of the unit cell density. A unit cell containing two acid molecules and one PBZT repeat unit has a calculated density of 1.995 g/cm³. This is significantly higher than the densities of MSA (1.483 g/cm³) and PBZT crystal (1.69 g/cm³¹⁰). Although the density of the ionic complex is expected to be higher than that of its neutral components, a more appropriate structure, having a stoichiometry of 4:1, is sought. This degree of protonation was brought out by the model calculations of the phase boundary, discussed above. Furthermore, gravimetric measurements of PBZT/Lewis acid complexes by Jehneke and co-workers^{3,4} showed a stoichiometry of 4:1. This stoichiometry in a unit cell yields a density of 2.83 g/cm³, which is prohibitively high. We therefore suggest that the actual unit cell, containing one PBZT repeat unit, is double the size of the calculated unit cell. With four MSA anions the unit cell density is 1.416 g/cm³, lower than that of MSA. Adding two more acid molecules raises the density to 1.833

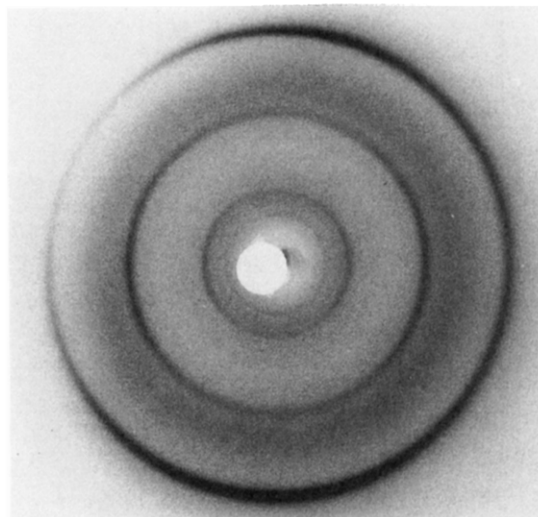


Figure 6. Diffraction pattern of the form I crystal solvate containing 20.3% (w/w) PBZT and 79.7% MSA heated to 150 °C.

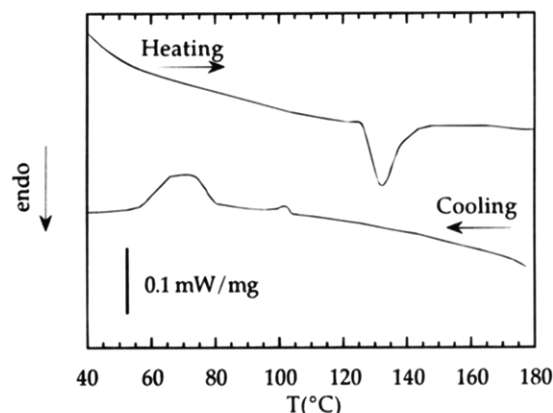


Figure 7. DSC traces of a sample containing 20.3% (w/w) PBZT and 79.7% MSA; heating and cooling cycles.

g/cm³, and the weight fraction of PBZT in the form I crystal solvate is 0.316.

Finally, we can infer on the basis of the experimental measurements a ternary phase diagram for the PBZT/MSA/water system, at 20 °C, which includes transitions between the isotropic and liquid crystal solutions and the crystal solvate forms I and II. This is shown in Figure 8 in terms of the weight fractions of water and PBZT. The solid lines in Figure 8 are the experimentally measured phase boundaries. These include the transition from isotropic to liquid crystal solution at low water content, the onset of precipitation of the form I phase from both isotropic and liquid crystal solutions, and the onset of transformation to the form II phase at low PBZT concentration. The dashed lines in Figure 8 are phase boundaries drawn in accordance with the Gibbs phase rule but have no experimental verification. The form I crystal solvate is taken as a stoichiometric complex of PBZT and MSA containing 32% PBZT, as discussed above. There is no information on the composition of the form II crystal solvate. It is described schematically as a region in the phase diagram containing about 4 MSA molecules per PBZT repeat unit and possibly a small amount of water. It should be noted that this diagram is characteristic of the particular PBZT molecular weight studied. Our experience suggests that transitions to the crystal solvate phases occur

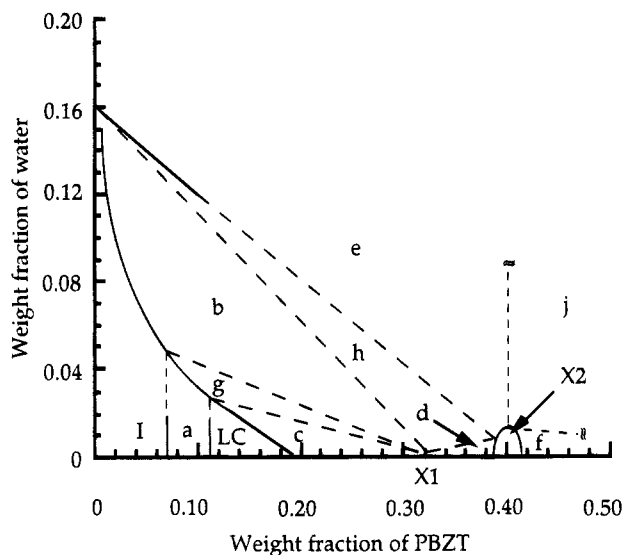


Figure 8. Ternary phase diagram for the PBZT/MSA/water system at 20 °C. Bold lines represent experimentally determined phase boundaries. Dashed lines are approximations drawn in accord with the phase rule. I, isotropic solution; LC, liquid crystal solution; X_1 , X_2 , form I and form II crystal solvates. Biphasic regions: (a) I + LC; (b) I + X_1 ; (c) LC + X_1 ; (d) X_1 + X_2 ; (e) I + X_2 ; (f) X_2 + polymer. Triphasic regions: (g) I + LC + X_1 ; (h) I + X_1 + X_2 ; (j) X_2 + polymer + water.

at lower water content as the molecular weight increases.

Conclusion

The role of water in inducing phase transformations in solutions of a rigid polymer in a strong acid was evaluated using quantitative measurements of dilute solutions of low molecular weight PBZT in MSA. Absorption of small amounts of moisture induce precipitation of the form I crystal solvate. Water deprotonates the free acid molecules in solution, producing more acid anions until the solubility product of the acid anions and protonated PBZT polycations is exceeded. Crystallization of the ionic PBZT/MSA complex, in a spherulitic manner, ensues. The results suggest that the form I crystal solvate contains 6 acid molecules per PBZT repeat unit, which has a degree of protonation of 4. At 20 °C, the form I phase is also obtained in dry MSA at a PBZT concentration about 20%. Transformation to the form II crystal solvate phase is induced by additional water uptake. The onset of the transition is related to deprotonation of the polymer following deprotonation of all the solvent molecules.

Acknowledgment. This project is supported by the U.S.–Israel Binational Science Foundation, which is

gratefully acknowledged. Financial support from the U.S. Air Force–E.O.A.R.D. and helpful interactions with scientists of the Polymer Branch, Wright Laboratories, are gratefully acknowledged.

References and Notes

- (1) Allen, S. R.; Filippov, A. G.; Farris, R. J.; Thomas, E. L.; Wong, C. P.; Berry, G. C.; Chenevey, E. C. *Macromolecules* **1981**, *14*, 1135.
- (2) Allen, S. R.; Filippov, A. G.; Farris, R. J.; Thomas, E. L. In *The Strength and Stiffness of Polymers*; Zachariades, A. E.; Porter, R. S., Eds.; Marcel Dekker: New York, 1983.
- (3) Jenekhe, S. A.; Johnson, P. O.; Agrawal, A. K. *Macromolecules* **1989**, *22*, 3216.
- (4) Jenekhe, S. A.; Johnson, P. O. *Macromolecules* **1990**, *23*, 4419.
- (5) Beltsios, K. G.; Carr, S. H. *J. Macromol. Sci. Phys.* **1990**, *B29*, 71.
- (6) Cohen, Y.; Thomas, E. L. *Polym. Eng. Sci.* **1985**, *25*, 1093.
- (7) Cohen, Y.; Thomas, E. L. *Macromolecules* **1988**, *21*, 433, 437.
- (8) Roche, E. J.; Takahashi, T.; Thomas, E. L. In *Fiber Diffraction Methods*; French, A. D.; Gardner, K. H., Eds.; ACS Symposium Series 141; American Chemical Society: Washington, DC 1980; Chapter 18.
- (9) Odell, J. A.; Keller, A.; Atkins, E. D. T.; Miles, M. J. *J. Mater. Sci.* **1981**, *16*, 3309.
- (10) Fratini, A. V. In *The Materials Science and Engineering of Rigid-Rod Polymers*; Adams, W. W., Eby, R. K., McLemore, D. E., Eds.; *Materials Research Society Symposium Proceedings* **1989**, *134*, 431.
- (11) Iovleva, M. M.; Papkov, S. P. *Polym. Sci. U.S.S.R. (Engl. Transl.)* **1982**, *24*, 236. Papkov, S. P. *Adv. Polym. Sci.* **1983**, *59*, 76.
- (12) Gardner, K. H.; Matheson, R. R.; Avakian, P.; Chia, Y. T.; Gierke, T. D. *Polym. Prepr. (Am. Chem. Soc., Div. Polym. Chem.)* **1984**, 91.
- (13) Frost, H. H. Microstructure and Phase Behavior of Poly(p-phenylene benzobisthiazole)Methane-sulfonic acid Crystal Solvates, M.Sc. Thesis, University of Massachusetts, Amherst, 1984.
- (14) Cohen, Y.; Frost, H. H.; Thomas, E. L. In *Reversible Polymeric Gels and Related Systems*; Russo, P. S., Ed.; ACS Symposium Series 350; American Chemical Society: Washington, DC, 1987; Chapter 12.
- (15) Cohen, Y. In *The Materials Science and Engineering of Rigid-Rod Polymers*; Adams, W. W., Eby, R. K., and McLemore, D. E., Eds.; *Materials Research Society Symposium Proceedings* **1989**, *134*, 195.
- (16) Cohen, Y.; Saruyama, Y.; Thomas, E. L. *Macromolecules* **1991**, *24*, 1161.
- (17) Cohen, Y.; Buchner, S.; Zachmann, H. G.; Davidov, D. *Polymer* **1992**, *33*, 3811.
- (18) Wolfe, J. F.; Loo, B. M.; Arnold, F. E. *Macromolecules* **1981**, *14*, 915.
- (19) Lee, C. C.; Chu, S. G.; Berry, G. C. *J. Polym. Sci., Polym. Phys. Ed.* **1983**, *21*, 1573.
- (20) Se, K.; Berry, G. C. In *Reversible Polymeric Gels and Related Systems*; Russo, P. S., Ed.; ACS Symposium Series 350; American Chemical Society: Washington, DC, 1987; Chapter 10.
- (21) Shen, D. Y.; Venkatesh, G. M.; Burchell, D. J.; Shu, P. H. C.; Hsu, S. L. *J. Polym. Sci., Polym. Phys. Ed.* **1982**, *20*, 509.

MA9461512